REPORT DOCUMENTATION PAGE

Form Approved OMB NO. 0704-0188

1. REPORT DATE (DD-MM-YYYY)	2. REPORT TYPE	3. DATES COVERED (From - To)
	New Reprint	-

4. TITLE AND SUBTITLE

Extending Mode Areas of Single-mode All-solid Photonic Bandgap Fibers

5a. CONTRACT NUMBER
W911NF-10-1-0423
5b. GRANT NUMBER
5c. PROGRAM ELEMENT NUMBER

6. AUTHORS

Guancheng Gu, Fanting Kong, Thomas W. Hawkins, Maxwell Jones, Liang Dong

5d. PROJECT NUMBER
5e. TASK NUMBER
5f. WORK UNIT NUMBER

7. PERFORMING ORGANIZATION NAMES AND ADDRESSES

Clemson University Research Foundation
Office of Sponsored Programs
Clemson University Research Foundation
Clemson, SC 29631 -0946

8. PERFORMING ORGANIZATION REPORT NUMBER

9. SPONSORING/MONITORING AGENCY NAME(S) AND ADDRESS (ES)

U.S. Army Research Office
P.O. Box 12211
Research Triangle Park, NC 27709-2211

10. SPONSOR/MONITOR'S ACRONYM(S)
ARO

11. SPONSOR/MONITOR'S REPORT NUMBER(S)
58391-EL-HEL.37

12. DISTRIBUTION AVAILIBILITY STATEMENT

Approved for public release; distribution is unlimited.

13. SUPPLEMENTARY NOTES

The views, opinions and/or findings contained in this report are those of the author(s) and should not contrued as an official Department of the Army position, policy or decision, unless so designated by other documentation.

14. ABSTRACT

Mode area scaling of optical fiber is highly desirable for high power fiber laser applications. It is well known that incorporation of additional smaller cores in the cladding can be used to resonantly outcouple higher-order modes from a main core to suppress higher-order-mode propagation in the main core. Using a novel design with multiple coupled smaller cores in the cladding, we have successfully demonstrated a singlemode

15. SUBJECT TERMS

fiber lasers, photonic bandgap fibers

16. SECURITY CLASSIFICATION OF:			17. LIMITATION OF ABSTRACT	15. NUMBER OF PAGES	19a. NAME OF RESPONSIBLE PERSON
a. REPORT	b. ABSTRACT	c. THIS PAGE			Liang Dong
UU	UU	UU	UU		19b. TELEPHONE NUMBER 864-656-5915

Report Title

Extending Mode Areas of Single-mode All-solid Photonic Bandgap Fibers

ABSTRACT

Mode area scaling of optical fiber is highly desirable for high power fiber laser applications. It is well known that incorporation of additional smaller cores in the cladding can be used to resonantly outcouple higher-order modes from a main core to suppress higher-order-mode propagation in the main core. Using a novel design with multiple coupled smaller cores in the cladding, we have successfully demonstrated a singlemode photonic bandgap fiber with record effective mode area of ~2650?m2. Detailed numeric studies have been conducted for multiple cladding designs. For the optimal designs, the simulated minimum higher-ordermode losses are well over two orders of magnitudes higher than that of fundamental mode when expressed in dBs. To our knowledge, this is the best higher-order-mode suppression ever found in fibers with this large effective mode areas. We have also experimentally validated one of the designs. M2<1.08 across the transmission band was demonstrated.

REPORT DOCUMENTATION PAGE (SF298)
(Continuation Sheet)

Continuation for Block 13

ARO Report Number 58391.37-EL-HEL
Extending Mode Areas of Single-mode All-solid ...

Block 13: Supplementary Note

Approved for public release; distribution is unlimited.

Extending mode areas of single-mode all-solid photonic bandgap fibers

Guancheng Gu, Fanting Kong, Thomas W. Hawkins, Maxwell Jones, and Liang Dong

Holcombe Department of Electrical and Computer Engineering, Clemson University, AMRL Building, 91 Technology Drive, Anderson SC 29625, USA

*ggu@g.clemson.edu

Abstract: Mode area scaling of optical fiber is highly desirable for high power fiber laser applications. It is well known that incorporation of additional smaller cores in the cladding can be used to resonantly out-couple higher-order modes from a main core to suppress higher-order-mode propagation in the main core. Using a novel design with multiple coupled smaller cores in the cladding, we have successfully demonstrated a single-mode photonic bandgap fiber with record effective mode area of ~2650μm^2. Detailed numeric studies have been conducted for multiple cladding designs. For the optimal designs, the simulated minimum higher-order-mode losses are well over two orders of magnitudes higher than that of fundamental mode when expressed in dBs. To our knowledge, this is the best higher-order-mode suppression ever found in fibers with this large effective mode areas. We have also experimentally validated one of the designs. M^2<1.08 across the transmission band was demonstrated.

OCIS codes: (060.2280) Fiber design and fabrication; (000.4430) Numerical approximation and analysis; (060.2270) Fiber characterization.

References and links

1. A. Tünnermann, T. Schreiber, and J. Limpert, "Fiber lasers and amplifiers: an ultrafast performance evolution," Appl. Opt. **49**(25), F71–F78 (2010).
2. D. J. Richardson, J. Nilsson, and W. A. Clarkson, "High power fiber lasers: current status and future perspectives [Invited]," J. Opt. Soc. Am. B **27**(11), B63–B92 (2010).
3. T. Eidam, S. Hanf, E. Seise, T. V. Andersen, T. Gabler, C. Wirth, T. Schreiber, J. Limpert, and A. Tünnermann, "Femtosecond fiber CPA system emitting 830 W average output power," Opt. Lett. **35**(2), 94–96 (2010).
4. F. Stutzki, F. Jansen, T. Eidam, A. Steinmetz, C. Jauregui, J. Limpert, and A. Tünnermann, "High average power large-pitch fiber amplifier with robust single-mode operation," Opt. Lett. **36**(5), 689–691 (2011).
5. T. Eidam, C. Wirth, C. Jauregui, F. Stutzki, F. Jansen, H. J. Otto, O. Schmidt, T. Schreiber, J. Limpert, and A. Tünnermann, "Experimental observations of the threshold-like onset of mode instabilities in high power fiber amplifiers," Opt. Express **19**(14), 13218–13224 (2011).
6. A. V. Smith and J. J. Smith, "Mode instability in high power fiber amplifiers," Opt. Express **19**(11), 10180–10192 (2011).
7. L. Dong, "Stimulated thermal Rayleigh scattering in optical fibers," Opt. Express **21**(3), 2642–2656 (2013).
8. J. Limpert, T. Schreiber, S. Nolte, H. Zellmer, T. Tunnermann, R. Iliew, F. Lederer, J. Broeng, G. Vienne, A. Petersson, and C. Jakobsen, "High-power air-clad large-mode-area photonic crystal fiber laser," Opt. Express **11**(7), 818–823 (2003).
9. J. Limpert, O. Schmidt, J. Rothhardt, F. Röser, T. Schreiber, A. Tünnermann, S. Ermeneux, P. Yvernault, and F. Salin, "Extended single-mode photonic crystal fiber lasers," Opt. Express **14**(7), 2715–2720 (2006).
10. L. Dong, T. Wu, H. McKay, L. Fu, J. Li, and H. G. Winful, "All-Glass Large-Core Leakage Channel Fibers," IEEE J. Sel. Top. Quantum Electron. **15**(1), 47–53 (2009).
11. G. Gu, F. Kong, T. W. Hawkins, P. Foy, K. Wei, B. Samson, and L. Dong, "Impact of fiber outer boundaries on leaky mode losses in leakage channel fibers," Opt. Express **21**(20), 24039–24048 (2013).
12. L. Dong, H. A. McKay, L. Fu, M. Ohta, A. Marcinkevicius, S. Suzuki, and M. E. Fermann, "Ytterbium-doped all glass leakage channel fibers with highly fluorine-doped silica pump cladding," Opt. Express **17**(11), 8962–8969 (2009).
13. F. Kong, G. Gu, T. W. Hawkins, J. Parsons, M. Jones, C. Dunn, M. T. Kalichevsky-Dong, K. Wei, B. Samson, and L. Dong, "Flat-top mode from a 50 μm-core Yb-doped leakage channel fiber," Opt. Express **21**(26), 32371–32376 (2013).

#230572 - $15.00 USD Received 11 Dec 2014; revised 16 Mar 2015; accepted 23 Mar 2015; published 2 Apr 2015

14. M. Kashiwagi, K. Saitoh, K. Takenaga, S. Tanigawa, S. Matsuo, and M. Fujimaki, "Effectively single-mode all-solid photonic bandgap fiber with large effective area and low bending loss for compact high-power all-fiber lasers," Opt. Express **20**(14), 15061–15070 (2012).
15. M. Kashiwagi, K. Saitoh, K. Takenaga, S. Tanigawa, S. Matsuo, and M. Fujimaki, "Low bending loss and effectively single-mode all-solid photonic bandgap fiber with an effective area of 650 μm2," Opt. Lett. **37**(8), 1292–1294 (2012).
16. S. Saitoh, K. Saitoh, M. Kashiwagi, S. Matsuo, and L. Dong, "Design Optimization of Large-Mode-Area All-Solid Photonic Bandgap Fibers for High-Power Laser Applications," J. Lightwave Technol. **32**(3), 440–449 (2014).
17. F. Kong, K. Saitoh, D. Mcclane, T. Hawkins, P. Foy, G. Gu, and L. Dong, "Mode area scaling with all-solid photonic bandgap fibers," Opt. Express **20**(24), 26363–26372 (2012).
18. G. Gu, F. Kong, T. Hawkins, J. Parsons, M. Jones, C. Dunn, M. T. Kalichevsky-Dong, K. Saitoh, and L. Dong, "Ytterbium-doped large-mode-area all-solid photonic bandgap fiber lasers," Opt. Express **22**(11), 13962–13968 (2014).
19. J. Fini, "Design of Solid and Microstructure Fibers for Suppression of Higher-Order Modes," Opt. Express **13**(9), 3477–3490 (2005).
20. X. Ma, C. H. Liu, G. Chang, and A. Galvanauskas, "Angular-momentum coupled optical waves in chirally-coupled-core fibers," Opt. Express **19**(27), 26515–26528 (2011).
21. J. M. Fini, J. W. Nicholson, R. S. Windeler, E. M. Monberg, L. Meng, B. Mangan, A. Desantolo, and F. V. DiMarcello, "Low-loss hollow-core fibers with improved single-modedness," Opt. Express **21**(5), 6233–6242 (2013).
22. J. M. Fini, B. Mangan, L. Meng, E. M. Monberg, J. W. Nicholson, and R. S. Windeler, "37-cell hollow-core-fiber designs with improved single-modedness," in CLEO: 2014 (OSA, 2014), p. SM1N.2.
23. T. Murao, K. Saitoh, and M. Koshiba, "Multiple resonant coupling mechanism for suppression of higher-order modes in all-solid photonic bandgap fibers with heterostructured cladding," Opt. Express **19**(3), 1713–1727 (2011).
24. A. Baz, L. Bigot, G. Bouwmans, and Y. Quiquempois, "Single-Mode, Large Mode Area, Solid-Core Photonic BandGap Fiber With Hetero-Structured Cladding," J. Lightwave Technol. **31**(5), 830–835 (2013).
25. A. W. Snyder and J. D. Love, *Optical Waveguide Theory* (Chaptman and Hall Ltd, 1983).
26. J. W. Nicholson, A. D. Yablon, J. M. Fini, and M. D. Mermelstein, "Measuring the Modal Content of Large-Mode-Area Fibers," IEEE J. Sel. Top. Quantum Electron. **15**(1), 61–70 (2009).
27. D. N. Schimpf, R. A. Barankov, and S. Ramachandran, "Cross-correlated (C^2) imaging of fiber and waveguide modes," Opt. Express **19**(14), 13008–13019 (2011).
28. F. Kong, G. Gu, T. W. Hawkins, J. Parsons, M. Jones, C. Dunn, M. T. Kalichevsky-Dong, S. P. Palese, E. Cheung, and L. Dong, "Quantitative mode quality characterization of fibers with extremely large mode areas by matched white-light interferometry," Opt. Express **22**(12), 14657–14665 (2014).

1. Introduction

In the course of developing high-power fiber lasers, mode area scaling is a key to mitigate nonlinear effects as a result of high optical intensity, such as stimulated Brillouin scattering (SBS), stimulated Raman scatting (SRS), Self-phase modulation (SPM) and four-wave mixing (FWM) [1,2]. In many applications, diffraction-limited beam is highly desired. We now know that mode instability can lead to poor mode quality at higher powers even in fibers with some higher-order-mode suppression [3–7]. To ensure single-mode output at high powers, very strong higher-order-mode suppression is also required along with the need for large effective mode areas.

In the recent decade, numerous approaches have been proposed, which led to a significant progress in mode area scaling of optical fibers. One notable area is in photonic crystal fibers (PCF) [3–5, 8, 9]. The short straight PCF rods used in the demonstrations have prevented their use in multi-kilowatts fiber lasers due to limited heat dissipation. The air holes in the cladding have also prevented them from being used in robust monolithic fiber lasers. The lack of strong higher-order-mode suppression has also led to mode instability issues [3–5]. To overcome some of the drawbacks, we have studied all-glass and coil-able leakage channel fibers (LCF) [10–13]. In the light of recent works in mode instabilities [6,7], much stronger higher-order-mode suppression is necessary to ensure single-mode operation at high powers.

Recently there have been significant interests in all-solid bandgap fibers (AS-PBF) [14–18]. The unique combination of an open cladding and a dispersive anti-resonant cladding which enhances the mode dependence enables some of the strongest higher-order-mode suppressions. In a recent work, we have demonstrated the existence of a robust single-mode

#230572 - $15.00 USD Received 11 Dec 2014; revised 16 Mar 2015; accepted 23 Mar 2015; published 2 Apr 2015

regime near the short-wavelength edge of the bandgap in an ytterbium-doped 50μm-core all-solid photonic bandgap fiber [18]. Our efforts in further mode area scaling of all-solid photonic bandgap fibers using similar designs have failed to find a design with sufficient higher-order-mode suppression for 100μm-core fibers. This led us to look for significant improvement in the designs.

It is well known that additional cores in the cladding which are in resonance for coupling with the higher-order modes in the main core can be used to suppress the higher-order modes in the main core [19,20]. This has even been recently used in hollow-core photonic bangap fibers for suppressing higher-order modes [21,22]. Recently, it has been suggested that multiple-coupled cores in the cladding can lead to much improved higher-order-mode suppression [23]. The key improvement is the use of multiple coupled small cores in the claddings which both enhances the coupling with higher-order modes in the main core and broadens the coupling resonance. The higher-order-mode in the main core is coupling to multiple coupled cores in the cladding simultaneously in the new design instead of just few isolated cores in the cladding in previous works. Narrow coupling resonance in the previous approaches [19,20] has always made them somewhat impractical. Such multiple coupled cores can be easily incorporated in the existing fabrication process of photonic bandgap fibers. The new proposal is, therefore, significant in providing a far more practical design. Recently, robust single-mode operation with mode field diameter of 44μm in a straight fiber was demonstrated using this approach in an all-solid photonic bandgap fiber [24].

In this work, we theoretically and experimentally investigated the multiple-cladding-resonance (MCR) designs in all-solid photonic bandgap fibers for further mode area scaling as well as for coiled operations. We have demonstrated robust single-mode operation with record effective mode area of ~2650 μm^2, i.e. a mode field diameter of 58μm, in straight fibers. This represents a significant improvement over previous demonstrations of robust single-mode operation in all-solid photonic bandgap fibers. Our simulation also indicates well over two orders of magnitude suppression of higher-order modes in coiled operations. This is the strongest higher-order-mode suppression at this large effective mode area to our knowledge.

2. Basic theory

Additional smaller cores can be easily created in the cladding of photonic bandgap fibers by missing several nodes. The smaller cores share the same cladding as the main core. If the cladding cores are well isolated, the resonant conditions between the fundamental mode in the cladding cores and various higher-order modes of the main core can be easily calculated. Using step-index fiber analogue, the propagation constant of modes in the main core can be written as

$$\beta_m^2 = k^2 n_b^2 - \frac{U_m^2}{\rho_m^2} \tag{1}$$

where k is the vacuum wavenumber; n_b is the refractive index of the background glass; ρ_m is the main core radius; and main core parameter U_m is as normally defined for optical fibers [25]. It needs to be noted that the refractive index of all the cores is the same as that of the background glass n_b in this case. Similarly, the propagation constant of modes in the cladding cores can be written as

$$\beta_c^2 = k^2 n_b^2 - \frac{U_c^2}{\rho_c^2} \tag{2}$$

The cladding core parameter U_c is defined similarly as U_m. The resonant condition for maximum coupling of a mode in the main core and a mode in the cladding core is $\beta_m = \beta_c$. Using the relations obtained thus far in Eq. (1) and Eq. (2), the resonant condition can be written as

#230572 - $15.00 USD Received 11 Dec 2014; revised 16 Mar 2015; accepted 23 Mar 2015; published 2 Apr 2015

$$\frac{U_m}{\rho_m} = \frac{U_c}{\rho_c} \tag{3}$$

Since the refractive index of core and cladding are the same for both main and cladding cores. The resonant condition can be rewritten using the normalized frequency, i.e. V value, V_m and V_c for the main and cladding cores respectively.

$$\frac{U_m}{V_m} = \frac{U_c}{V_c} \tag{4}$$

This can be easily calculated for the fundamental mode of the cores in the cladding and various higher-order modes in the main core (see Fig. 1).

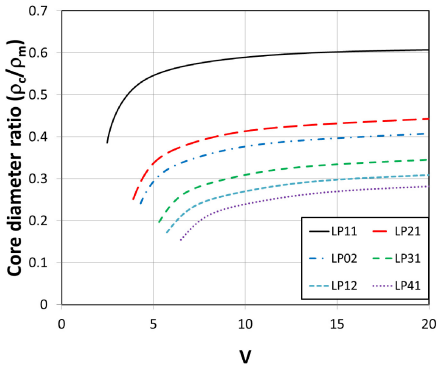

Fig. 1. Required core diameter ratio (ρ_c/ρ_m) for maximum resonant coupling between the fundamental mode of the cladding core and one of the higher-order modes of the main core versus normalized frequency (V value) of the main core.

The horizontal axis is the V value of the main core. For weakly coupled cladding cores, Fig. 1 provides a reasonable approximations for a straight fiber. In the multimode regime with V>10, for coupling with LP_{11} and LP_{21} modes in the main core, $\rho_c/\rho_m \approx 0.6$ and 0.44 respectively. As it turned out, this approximation works reasonably well for cladding cores of a photonic bandgap fibers.

3. FEM simulations

Based on the approximation in Fig. 1 as guidance, three cladding designs were numerically studied using a FEM mode solver. The cross-sections of all designs are shown in Fig. 2. For all the designs, a 7-cell core is adopted. Instead of the periodically arranged high-index inclusions surrounding the core, several cladding structures are used to form the cladding. The smaller cores in the cladding are formed by purposefully taking out a certain number of nodes such that a cladding defect core is created. The first design shown in the left side of Fig. 1 is referred to the "mixed-cell" since it has two and three nodes removed to create the cladding cores. The second and third design shown in the middle and right side of the Fig. 2 are accordingly referred to "three-cell" and "two-cell" respectively. The core diameter ratio $\rho_c/\rho_m \approx 0.65$ and 0.53 for the 3- and 2-cell cores respectively, close to the 0.6 required in Fig. 1 for coupling with LP_{11} mode in the main core. It is worth noting that the effective mode index of the cladding core will increase or decrease in a coiled fiber depending on its relative location to the center of the coil. The condition required in Eq. (4) is, therefore, only an approximation in this case.

The nodes in the cladding were made of germanium-doped silica with a graded index profile similar to the one used in our previous Yb-doped PBF [17,18]. The pitch, that is the

#230572 - $15.00 USD Received 11 Dec 2014; revised 16 Mar 2015; accepted 23 Mar 2015; published 2 Apr 2015

distance between two adjacent cladding nodes, is 25μm, which yields a 100μm core diameter. The ratio between the diameter of the cladding nodes and pitch is fixed, at 0.24.

A commercially available COMSOL Finite Element Method (FEM) mode solver is used for the simulation. A perfectly matched layer is implemented to obtain the mode loss. The fiber is simulated under 50cm bending radius. This provides a coil diameter which is acceptable for multi-kw high-power fiber lasers and minimizes mode compression due to coiling. The wavelength is scanned from 900nm to 1100nm. Given the symmetry of the cladding arrangement, propagation loss under different bending orientations has been studied. The arrow in the inset of Fig. 3 indicates the direction where the center of the coil is. The loss curves with respect to the wavelength are plotted in Fig. 3.

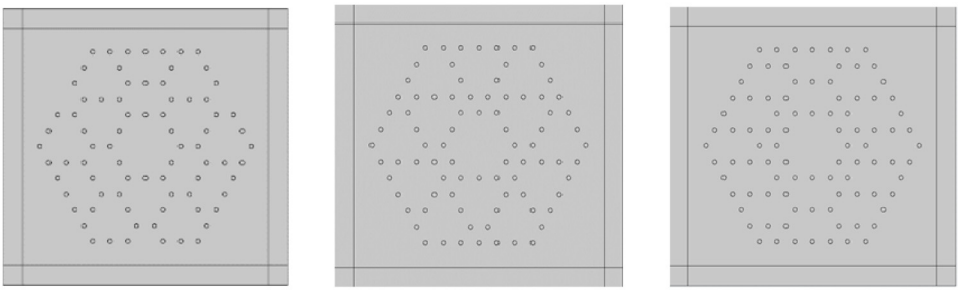

Fig. 2. Cross-section of PBFs studied. From left to right are: mixed-cell, three-cell and two-cell AS-PBF.

For the mixed-cell PBF (Fig. 3(a)) and three-cell PBF (Fig. 3(c)), each has three possible different bending orientations: one horizontal and two vertical. Meanwhile two-cell PBF only has two fundamentally different ways to coil. The first three dominant modes, namely LP_{01} and LP_{11} (LP_{11A} and LP_{11B}) with two orthogonal orientations are presented. The inset in Fig. 3(a) shows the generic mode pattern for LP_{01}, LP_{11A} and LP_{11B}. It can be clearly seen that when fiber is bent horizontally, all three designs demonstrate significant differential mode loss within the third bandgap at wavelength ranging from 1000nm to 1030nm, which indicates a possible window for single-mode operation. The lowest fundamental mode loss can be as low as ~0.01dB/m.

One should note that at 1030nm the FM tends to have a small loss peak, which can be attributed to the resonance effect with the cladding, as it can be clearly seen in the inset of Fig. 3(a). The differential loss is much worse when bending vertically. For example, for the three cell PBF shown in the Fig. 3(c), the LP_{11A} mode has almost the same loss as LP_{01} mode does. At longer wavelengths, it can even have less loss than LP_{01} mode. The loss of all LP modes tend to increase significantly outside the bandgap when the wavelength is below 1000nm or beyond 1050nm. The mode can be severely distorted in the high loss regime.

Table 1. Summary of loss ratio for three types of fiber design

Fiber Type	Wavelength (nm)	Minimum FM loss (dB/m)	Corresponding HOM loss (dB/m)	Loss ratio
Mixed-cell	1020	0.02	3.83	192
Three-cell	1040	0.01	4.13	413
Two-cell	1000	0.02	5.03	252

Table 1 summarized the FM loss, minimum HOM loss and loss ratios at the wavelength that has the minimum FM loss for the horizontally coiled fibers. Note that the corresponding HOM loss is picked between LP_{11A} and LP_{11B}, whichever has the lower loss. From the table, it can be seen that the three-cell PBF has the highest loss ratio at 1040nm but the bandwidth for low FM loss is rather narrow in this case. The two-cell PBF has the second highest loss ratio, yet the LP_{11} mode loss drops down dramatically once the wavelength is longer than 1000nm.

#230572 - $15.00 USD Received 11 Dec 2014; revised 16 Mar 2015; accepted 23 Mar 2015; published 2 Apr 2015

It is worth noting that, as for the mixed-cell fiber design under horizontal bending, both LP_{11A} and LP_{11B} mode loss are above 10dB/m while the fundamental mode loss is kept at or below 0.2dB/m around 1000nm. In addition, the bandwidth for such high differential loss is broader compared to the three-cell and two-cell designs. As the wavelength move toward 1020nm, the LP_{01} continues to drop below 0.1dB/m, even though the LP_{11A} mode loss simultaneously decreases, the loss ratio between the LP_{11} to LP_{01} still reaches as high as 192 (see Table 1.).

Ideally, the bending orientation should be controlled to be horizontal for best HOM suppression. However, in practical cases, the bending direction may be arbitrary, meaning a fiber can have a combination of all the possible bending orientations throughout its length. In this case, total HOM loss will be an average loss of all the orientations. Since FM loss remains largely independent of the orientations, it is still sufficient to realize single transverse-mode operation over a few meters of fiber although with a lesser HOM suppression.

4. Experiments

To validate the simulation, the mixed-cell design was fabricated through standard stack-and-draw process. The dimension of the fiber is illustrated in Table 2. and the cross-section of the actual fiber is shown in Fig. 4. One can notice that there is a slight difference between actual dimension and numeric simulation, which can be attributed to parameter control during the fabrication. The germanium nodes in the cladding have the same refractive index profile as the one used in the simulation. The center core is made of silica. The outer shape of the fiber is rounded hexagon, which also helps increase the differential mode loss [11].

Table 2. Dimensions of Fabricated hetero-structured PBF

Pitch/Λ (μm)	Node Size/d (μm)	d/Λ	Core size flat to flat (μm)	Core size corner to corner (μm)	OD flat-to-flat (μm)	OD corner-to-corner (μm)
24.8	6.6	0.27	82.3	91.7	411.1	421.3

Transmission, mode pattern and beam quality of the mixed-cell PBF have been fully characterized. In all measurements, the fiber is bent at diameter of 1m, conforming to the bending radius set in the numeric simulation. It is also worth mentioning that the bending direction was not controlled during the measurement. The transmission of a 4m PBF is shown in Fig. 5 in a linear scale. The scanning wavelength ranges from 998nm to 1041nm. The highest transmission peak is observed at the vicinity of 1015nm. Knowing the dimension difference, this is well correspondent to the computational results, which has low attenuation around 1020nm under all three bending configuration.

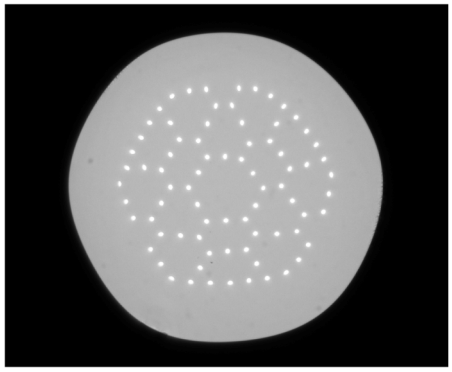

Fig. 3. Cross-section of the fabricated mixed-cell PBF.

#230572 - $15.00 USD Received 11 Dec 2014; revised 16 Mar 2015; accepted 23 Mar 2015; published 2 Apr 2015

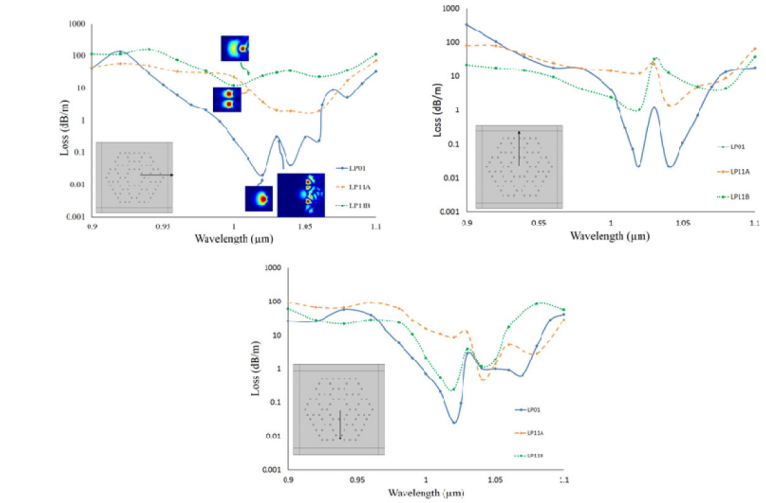

(a)

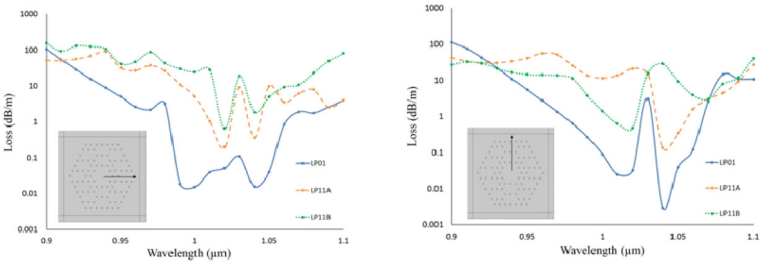

(b)

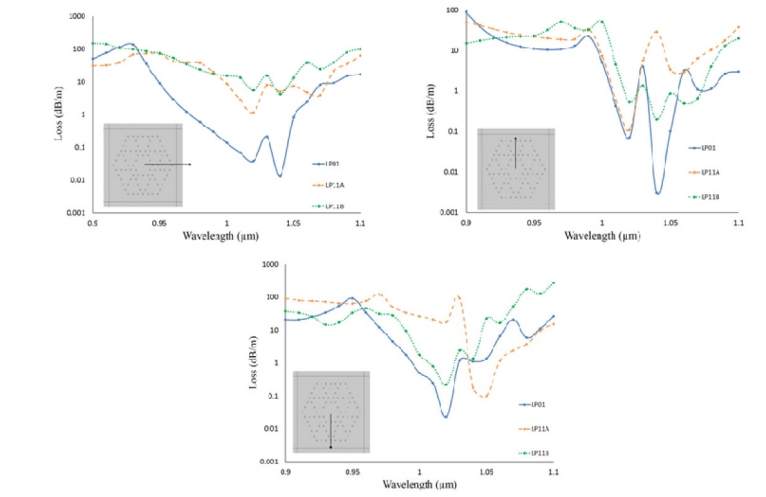

(c)

Fig. 4. Simulated loss of LP_{01} (blue) and LP_{11} modes (Orange and Green) in (a) mixed-cell design, (b) two-cell design and (c) three-cell design. The insets show the layout of different cladding arrangement. The arrow in the inset indicates the coil center. Insets also show the mode patterns of LP_{01} and LP_{11}.

#230572 - $15.00 USD Received 11 Dec 2014; revised 16 Mar 2015; accepted 23 Mar 2015; published 2 Apr 2015

The simulated effective mode area (EMA) of the fiber versus bending diameter is shown in Fig. 6. At bending diameter of 1m, the EMA is ~1842μm^2, marked by the orange diamond in Fig. 6.

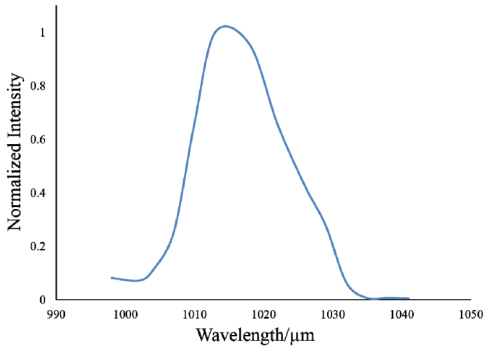

Fig. 5. Normalized Transmission of 4m of the fabricated PBF.

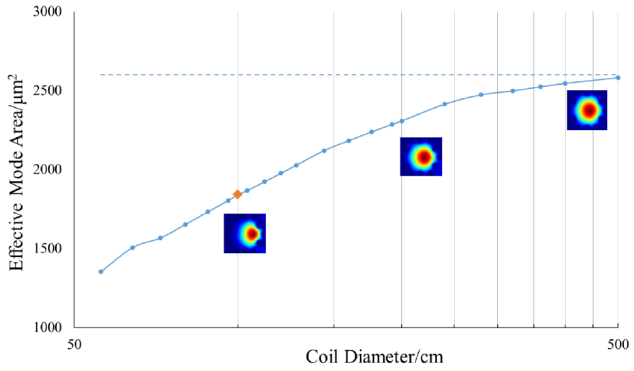

Fig. 6. Estimated effective mode area (EMA) of the fabricate PBF. The coil diameter is in log scale. The insets are mode patterns under different coil diameters. At 1m bending diameter, the EMA is estimated to be ~1842μm^2, shown as the orange diamond in the chart. The dash line indicates the EMA of a straight fiber.

At large core diameters as in the fabricated fibers in this work, the effective mode indexes of the fundamental and higher-order modes are very close, leading to small intermodal delays. This causes significant difficulty in using the well-known quantitative mode characterization techniques such as S^2 and C^2 techniques [26, 27]. Much wide wavelength scan range is required for the S^2 method. In case of the C^2 method, broadband source with coherent length less than few tens of femtosecond is required, in addition to the necessary dispersion compensation. Recently we have demonstrated the first quantitative mode characterization in a 100μm-core fiber using a matched white-light interferometry where dispersion is completely compensated [28]. The fabricated fiber in this work, however, has very narrow transmission band, which makes any quantitative mode characterization impossible.

To verify the robustness of single-mode operation, a tunable laser light was launched into a 4m PBF bending at 1m diameter. The fiber was initially aligned such that light could be directly launched into the center core while the tunable laser scanned the wavelength from 1010nm to 1030nm at the increment of 5nm. The near field mode pattern was captured using a CCD camera at the other end of the PBF. Then the fiber was moved off the optimal launching condition by 12μm, 24μm and 36μm sequentially in attempt to excite HOM. After each offset, the tunable laser would repeat the same wavelength scan.

#230572 - $15.00 USD Received 11 Dec 2014; revised 16 Mar 2015; accepted 23 Mar 2015; published 2 Apr 2015

Figure 7 shows the near field mode image under different launching conditions at various wavelengths. At the optimal launching condition, the fundamental mode was well guided from 1010nm to 1015nm and start to degrade slightly at 1030nm. The HOM was constantly absent across the wavelength spectrum as the launching condition was gradually deteriorated from the optimal launching position. This measurement effectively demonstrated the single-mode operation for this PBF.

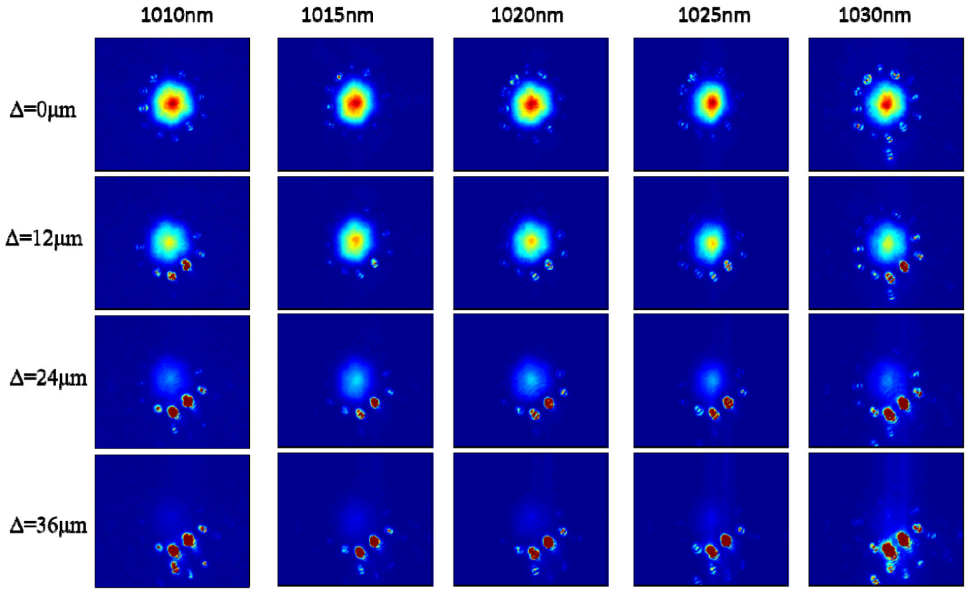

Fig. 7. Near filed mode pattern of the mixed-cell PBF at various wavelengths. Δ is the distance of the launch offset.

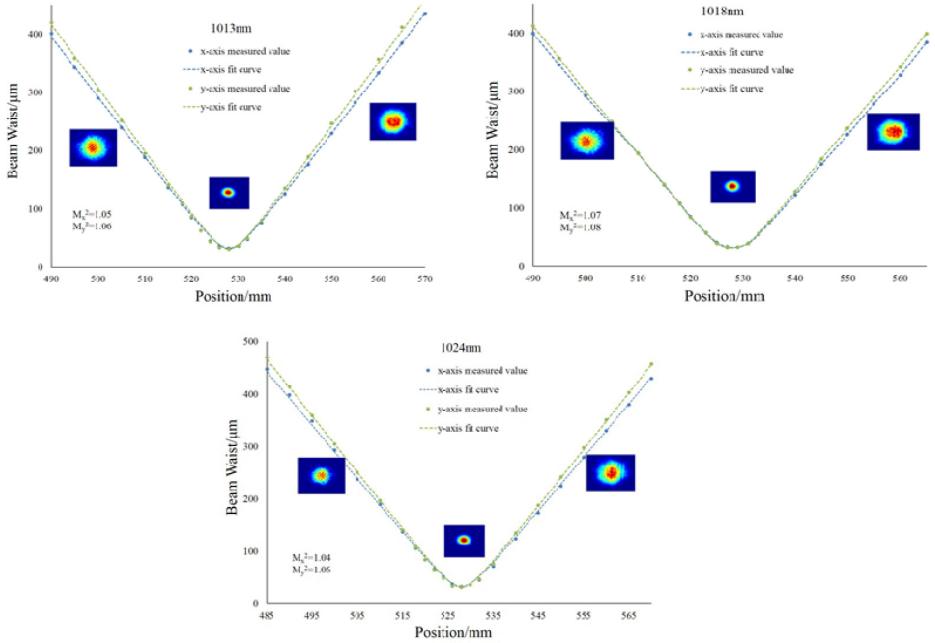

Fig. 8. Beam quality measurement at wavelength of 1013nm, 1018nm and 1024nm. Both x-axis (blue) and y-axis (green) were measured with selected mode profiles along the curve.

#230572 - $15.00 USD Received 11 Dec 2014; revised 16 Mar 2015; accepted 23 Mar 2015; published 2 Apr 2015

The beam quality was further verified by employing M^2 technique. Three wavelengths from the tunable laser, namely 1013nm, 1018nm and 1024nm were selected for this measurement. The fiber length and coil diameter are the same as the ones in the tests mentioned above. A CCD camera is deployed to trace the propagation of the output beam. The results are shown in Fig. 8. It can be seen that for all the three wavelengths, the measured M^2 values along the horizontal and vertical direction are equal or less than 1.08. The beam profiles captured also indicate a good single-mode operation. This further confirms that robust single-mode operation is supported in the large core while HOM is highly suppressed by the outer cladding defects due to coupling.

5. Conclusion

In summary, we have demonstrated robust single-mode operation in a MCR-PBF with a record mode area of ~2650μm^2. Three types cladding layouts have been theoretically studied. Comparing among different bending orientations, horizontal bending performs much better in terms of differential mode loss than that vertical bending does. With controlled bending configuration, a very high loss ratio between LP_{11} and LP_{01} can be realized. Mixed-cell design was fabricated and demonstrated to be robustly single-mode at coil diameter of 1m. The M^2 was measured to be less than 1.08 across the bandgap. This work further pushes mode area scaling limit in single-mode all-solid photonic bandgap fibers. The MCR mechanism can be potentially adopted to realize rare-earth doped single-mode fiber lasers with 100μm core diameter.

Acknowledgment

This material is based upon work supported in part by the U. S. Army Research Laboratory and the U. S. Army Research Office under contract/grant number W911NF-10-1-0423 through a Joint Technology Office MRI program.

#230572 - $15.00 USD Received 11 Dec 2014; revised 16 Mar 2015; accepted 23 Mar 2015; published 2 Apr 2015